



# Nuclear-Polarized Phases of H Atoms Embedded in Solid Molecular Hydrogen Films

S. Sheludiakov<sup>1,2</sup>  · D. M. Lee<sup>1</sup> · V. V. Khmelenko<sup>1</sup> · J. Ahokas<sup>3</sup> · J. Järvinen<sup>3</sup> · S. Vasiliev<sup>3</sup>

Received: 29 June 2021 / Accepted: 25 August 2021

© The Author(s), under exclusive licence to Springer Science+Business Media, LLC, part of Springer Nature 2021

## Abstract

We report on an electron-spin resonance study of nuclear-polarized phases of hydrogen atoms embedded in solid H<sub>2</sub> films at temperatures 0.1–1.5 K and a high magnetic field of 4.6 T. The H atoms in solid H<sub>2</sub> were generated by two different dissociation techniques: a cryogenic rf-discharge and bombardment by 5.7 keV electrons via tritium decay. In both studies, we observed a build-up of a spontaneous nuclear-polarized phase (SNPP,  $p=0.35$ ) at temperatures below  $\sim 0.8$  K similar to that reported in our previous work. We were also able to create a highly nuclear-polarized phase (HNPP,  $p \simeq 0.75$ ) using Dynamic Nuclear Polarization for samples exposed to a cryogenic rf discharge, whereas we failed to obtain this phase for the samples bombarded by 5.7 keV electrons. We suggest that failing to achieve the HNPP in the samples exposed to high-energy electrons released during tritium decay may be explained by an effect of faster nuclear relaxation stimulated by electrons bombarding the H<sub>2</sub> matrix and rapidly relaxing centers in the film substrate created during accumulation of H atoms in solid H<sub>2</sub>.

**Keywords** Hydrogen atoms · Solid molecular hydrogen · Nuclear polarization

---

✉ S. Sheludiakov  
ses276@pitt.edu

<sup>1</sup> Institute for Quantum Science and Engineering, Department of Physics and Astronomy, Texas A&M University, College Station, TX 77843, USA

<sup>2</sup> Present Address: Department of Physics and Astronomy, University of Pittsburgh, Pittsburgh, PA 15260, USA

<sup>3</sup> Department of Physics and Astronomy, University of Turku, 20014 Turku, Finland

## 1 Introduction

Solid molecular hydrogen along with the helium solids represent a special class of so-called quantum crystals. Similar to the solid helium isotopes where He atoms remain essentially delocalized, light atomic impurities, H, embedded in solid molecular hydrogen travel through the matrix by a repetition of exchange tunneling reaction  $H+H_2 \rightarrow H_2+H$  at temperatures even below 1 K [1–7]. A number of phenomena related to the exchange interaction or Bose-Einstein condensation (BEC) of H atoms in solid  $H_2$  might be expected at a high enough H atom concentrations and low temperatures. In contrast to solid  $^4\text{He}$ , however, the properties of H atoms in solid  $H_2$  and their ground state population can be probed directly using the methods of magnetic resonance.

In a series of studies, Ahokas et al. [8, 9] and Järvinen et al. [10] observed a large excess of nuclear polarization,  $p=(n_a - n_b)/(n_a+n_b)$ , of H atoms trapped in a solid  $H_2$  matrix over the values predicted by the Boltzmann statistics, with  $n_a$  and  $n_b$  being the populations of the  $|a\rangle$  and  $|b\rangle$  states of H atoms (Fig. 1A). A substantial overpopulation of the ground  $|a\rangle$ -state was observed for the samples where the  $H_2$  matrix and the embedded H atoms were created by different deposition and dissociation techniques: ultra-slow deposition of the products of H atom three-body recombination in the gas phase [8] and electron-impact dissociation of  $H_2$  molecules in solid hydrogen films by running a cryogenic rf discharge in the sample cell [9, 10]. These results were analyzed by Mueller and Hazzard [11] who examined several possible mechanisms for the build-up of a large non-Boltzmann nuclear polarization, including the possibility of a local BEC of H atoms in solid  $H_2$ . The exotic supersolid state was long sought for vacancies in solid  $^4\text{He}$  [12–14] but was finally obtained for assemblies of ultra-cold atoms in optical traps [15–18]. Nevertheless, none of the mechanisms for large non-Boltzmann population of H atoms in solid  $H_2$  suggested in [11] were able to fully explain all the phenomena observed in Refs. [8, 9].

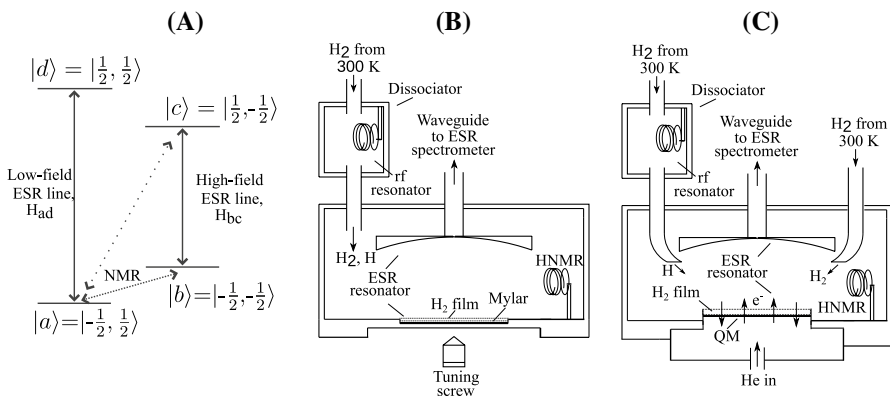


**Fig. 1** A H atom energy level diagram in high magnetic field. The nuclear and electron spin states are labeled as  $|m_s, m_I\rangle$ . The allowed transitions are shown by solid arrows, the forbidden transition is shown by a dotted line. **B, C** The schematic of sample cells used in experiments in Texas A&M University and the University of Turku, respectively

In our recent work [19], we observed formation of two stable phases where the nuclear polarization of H atoms in solid  $\mu\text{m}$ -thick  $\text{H}_2$  films significantly exceeded the values dictated by the Boltzmann statistics. The first phase, the spontaneously nuclear polarized phase (SNPP) with  $p \simeq 0.35$ , developed spontaneously during sample storage in high magnetic field ( $B=4.6$  T) at  $T < 0.8$  K over 5–7 days (about 120–170 h). The second phase, the highly nuclear-polarized phase (HNPP), with  $p=0.75$ , was achieved at  $T < 0.55$  K by using sequences of Dynamic Nuclear Polarization (DNP) followed by relaxation of the nuclear polarization. Each such saturation-relaxation sequence (SRS) included application of the Overhauser effect DNP, which involves saturation of the  $b - c$  ESR line followed by cross-relaxation to the  $a$ -state [19, 20] (see Fig. 1A), and a following polarization relaxation to an asymptotic value. We, however, failed to obtain high nuclear polarization for H atoms in the regions of  $\text{H}_2$  with their low concentrations,  $[\text{H}] < 10^{18} \text{cm}^{-3}$ , as well as in annealed  $\text{H}_2$  films. Moreover, we did not observe enhanced nuclear polarization of H atoms in solid HD [21].

We considered three possible mechanisms for the nuclear polarization build-up: statistical correlations between identical bosonic H atoms, magnetic ordering of their nuclear spins, and the H atom nuclear spin alignment due to formation and following dissociation of weakly bound  $^3\Sigma_u^+ \text{H}_2$  molecules [19].

In the present work, we aimed at providing further insight into the formation of the polarized phases of H atoms. We carried out an ESR study of H atoms in solid  $\text{H}_2$  films at  $T=0.1$ – $1.5$  K and in a high magnetic field of 4.6 T utilizing two setups with different techniques for an *in situ* dissociation of  $\text{H}_2$  molecules in solid molecular hydrogen films. The H atoms in the solid  $\text{H}_2$  matrix for the first type of samples, studied at the Texas A&M University, were generated by running an rf-discharge in He vapor above the  $\text{H}_2$  film. For the second type, studied at the University of Turku, the H atoms were produced by a continuous bombardment of  $\text{H}_2$  films by 5.7 keV electrons released during  $\beta$ -decay of tritium trapped in the sample cell walls while having no helium gas in the sample cell. It turned out that for the latter type of H– $\text{H}_2$  samples, once formed at the level of  $p=0.35$ , the SNPP experienced a slow, but steady decline on a time scale of weeks. We were also unable to achieve the HNPP for these samples. In addition to that, we did not observe any deviation from the Boltzmann statistics for the 160 nm thick  $\text{H}_2$  Turku sample. We provide possible explanations for these observations.

## 2 Experimental Details

The experiments were carried out using two experimental setups located at the University of Turku and Texas A&M University. Both setups are based on commercial dilution refrigerators, Oxford 2000 and Oxford 200, respectively. The sample cells (SCs) are located in the centers of 4.6 T superconducting magnets and attached to the mixing chambers of dilution units to provide sufficient cooling. The SCs had similar designs as presented schematically in Fig. 1B and C. The main diagnostic tools in both apparatuses are cryogenic 128 GHz heterodyne Electron Spin Resonance (ESR) spectrometers with a sensitivity of  $\sim 10^{10}$  spins [22]. The ESR

resonators have an open Fabry–Perot design which made it possible to arrange auxiliary rf resonators tuned to the  $H_{ab}$  NMR transition frequency,  $f=910$  MHz, labeled as HNMR in Fig. 1B and C.

The top mirrors of both ESR resonators are made of copper and have a spherical shape. The  $400\mu\text{m}$  thick palladium (Pd) bottom mirror of the Turku cell (Fig. 1C) also serves as a top electrode of the quartz microbalance (QM) which enabled a simultaneous measurement of the  $\text{H}_2$  film thickness and the ESR signals of H atoms embedded in the  $\text{H}_2$  film [23]. The bottom flat mirror of the Texas cell is made of oxygen-free copper and covered with a  $\approx 20\mu\text{m}$  thick Mylar foil [10] (Fig. 1B).

The main differences between the two experiments appear in the procedures for depositing solid  $\text{H}_2$  films and dissociating  $\text{H}_2$  molecules. The Texas experiment was focused on studying thick,  $10\text{--}100\mu\text{m}$ ,  $\text{H}_2$  films created by solidifying molecular hydrogen from the liquid phase [10, 19]. Prior to that, the  $\text{H}_2$  gas was condensed into the SC from a room temperature gas handling system keeping the sample cell at temperatures of  $15\text{--}20$  K. Molecular hydrogen condensed into a macroscopic film at the cell bottom and then solidified, forming a thick film of solid  $\text{H}_2$  on the flat mirror of the ESR resonator. Then the cell was slowly cooled down to  $T \approx 0.5\text{--}0.7$  K and a small amount,  $\sim 1\mu\text{mole}$ , of He gas was condensed into the SC in order to run the rf discharge in the helium vapors by using the HNMR resonator. The electrons created during the discharge dissociate a fraction of the  $\text{H}_2$  molecules in the solid film. The H atoms, in this case, are generated in a rather shallow surface layer of  $\approx 100$  nm [23]. The discharge is stopped when the local concentrations of H atoms in solid  $\text{H}_2$  level off at the value of  $\approx 10^{19}\text{cm}^{-3}$ .

The solid  $\text{H}_2$  films created in Turku were much thinner,  $0.05\text{--}2.5\mu\text{m}$ . The films were quench condensed onto the QM surface directly from the room-temperature gas-handling system or from the cold dissociator chamber. The QM temperature during the  $\text{H}_2$  film deposition was stabilized at  $T \approx 0.7\text{--}1.3$  K. The Turku SC was also used in our previous experiments with solid tritium films [24] and a number of tritium atoms and molecules remained trapped in the ESR resonator mirrors and in the SC walls. These  $\beta$ -decaying tritium atoms and molecules worked as a permanent source of electrons with an average energy of  $5.7$  keV which penetrated through the whole  $\text{H}_2$  film and dissociated the  $\text{H}_2$  molecules there rather uniformly. The dissociation of  $\text{H}_2$  molecules in the Turku samples took place continuously and could not have been interrupted during sample storage. Each electron released in an event of tritium  $\beta$ -decay produces about 50 H atoms in the  $\text{H}_2$  films [24]. Based on the H atom accumulation rate we concluded that of order  $10^{16}$  tritium atoms are trapped in the sample cell walls. This corresponds to an accumulation rate of H atoms in solid  $\text{H}_2$  films of order  $\approx 2 \times 10^9\text{s}^{-1}$ .

The upper energy levels of H atoms,  $|c\rangle$  and  $|d\rangle$ , in the high magnetic field of our experiments,  $B=4.6$  T, remain unoccupied up to temperatures of  $T \approx 1.5$  K. Therefore, the  $H_{ad}$  and  $H_{bc}$  ESR line areas are proportional to the populations,  $n_a$  and  $n_b$ , of the two lower hyperfine levels,  $|a\rangle$  and  $|b\rangle$  (Fig. 1A).

A special chamber, the  $\text{H}_2$  dissociator, was arranged above the main volumes of both sample cells in order to provide a flux of H atoms in the gas phase created by running the rf discharge there. The ESR lines of atomic hydrogen gas collected in

the SC were used as a reference for determination of the spectroscopic parameters and average concentrations of H atoms embedded in solid H<sub>2</sub> films [9]. The local H atom concentrations in both studies were determined based on the concentration-dependent ESR line broadening due to dipolar interaction between the H atom electron spins [9].

### 3 Experimental Results

In this work, we aimed to provide a further insight into nuclear-polarized phases, the SNPP and HNPP, observed in our previous studies. In this section, we present a detailed study of the effects of temperature, magnetic field, and substrate on nuclear polarization in these two types of samples to understand their different behavior. We use a notation of TXS for the samples studied in the present work in Texas and TUS for those studied in the present work in Turku.

#### 3.1 Effect of Storage Time

We studied three TUS H<sub>2</sub> samples prepared from the hydrogen gas with a normal ortho-para composition (75% ortho, 25% para H<sub>2</sub>). The measurement was begun right after finishing deposition of a 2.5 μm H<sub>2</sub> film onto the QM and stabilizing the SC temperature at  $T=0.15$  K. In addition to the H<sub>2</sub> films deposited onto a bare Pd mirror, we also studied a 2.5 μm H<sub>2</sub> film deposited onto the QM preplated with a 2.5 μm Ne film. The neon film bombarded by the electrons released during tritium decay provided a flux of secondary electrons [25] which accelerated accumulation of H atoms in the H<sub>2</sub> film. We monitored evolution of the H atom nuclear polarization at this temperature for about 3.5 weeks. The doublet of H atom ESR lines separated by 507 G appeared within about 10 minutes after finishing film deposition. The H atom concentration approached  $\approx 1 \times 10^{19} \text{ cm}^{-3}$  after about two weeks of sample storage at  $T=0.15$  K (red squares in Fig. 2A). The ESR lines of H atoms had a regular homogeneously broadened Lorentzian shape with a dipolar contribution to the linewidth  $\approx 1.5$  G (Fig 2B). The H<sub>ad</sub> ESR line also acquired additional broadening due to a resonant interaction of the like H atoms in the ground  $|a\rangle$ -state [9, 26]. The ESR signals from H atoms embedded in solid Ne were about 30 times weaker than those of H in the H<sub>2</sub> film.

The nuclear polarization of H atoms in this sample involving the neon substrate increased continuously in the first three days of storage and then leveled off at a maximum value  $p \approx 0.42$  (blue circles in Fig. 2A). However, after passing the maximum, it began to decrease and approached an asymptotic value of  $p \approx 0.35$ , which is far above the nuclear spin polarization at this temperature,  $p=0.15$ , dictated by Boltzmann statistics. This asymptotic value of nuclear polarization matches the one observed for the SNPP in our recent work in Texas [19].

After measuring the polarization decline for about ten days, we *saturated* the H<sub>ab</sub> NMR transition to equalize the populations of  $|a\rangle$  and  $|b\rangle$  states and then measured

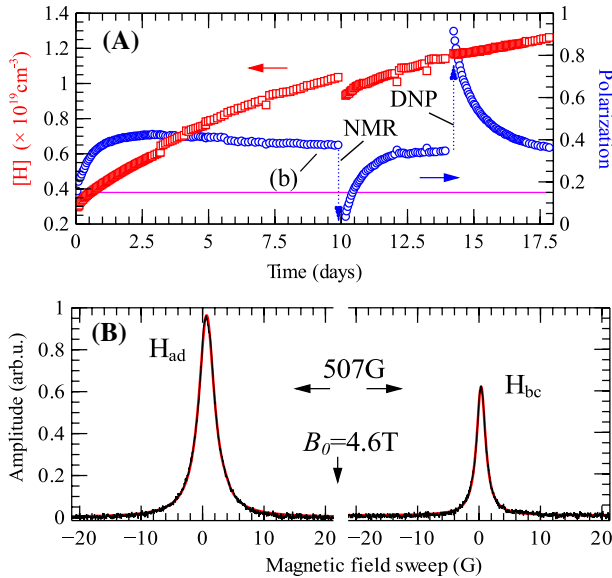


**Fig. 2** **A** Time evolution of the H atom concentration in a  $2.5\mu\text{m}$   $\text{H}_2$  film on  $2.5\mu\text{m}$  solid Ne film (open red squares) stored at  $T=0.15$  K and dependence of the H atom nuclear polarization on time (blue circles) measured in Turku. The value of the nuclear polarization,  $p=0.15$ , for the Boltzmann occupation of the  $|a\rangle$  and  $|b\rangle$  states is shown by a solid magenta line. **B** The  $\text{H}_{ad}$  and  $\text{H}_{bc}$  ESR lines for the same sample measured at a time specified as **(B)** in **(A)** when the SNPP was achieved. The very small contributions to the ESR signals from the H atoms trapped in solid Ne were subtracted for convenience. The fitting lines are shown by red lines in **(B)** (Color figure online)

the polarization recovery (Fig. 2A). The polarization recovery was fitted with an exponential function,  $p(t)=p-a \cdot \exp(-T_{1N}/t)$ , where  $p$  is an asymptotic polarization,  $T_{1N}$  is the nuclear spin-lattice relaxation time and  $a$  is a free fitting parameter. The nuclear polarization recovered back to  $p=0.35$  with a characteristic time  $T_{1N}$  equal to 1 day.

As a next step, we tried to stimulate the nuclear polarization build-up by using saturation-relaxation sequences (SRSs) to examine the possibility of creating the HNPP in this type of H- $\text{H}_2$  sample. The polarization relaxation was analyzed using the same exponential function,  $p(t)$ , described above. We found that after applying DNP, the nuclear polarization reverted to the same asymptotic value of  $p=0.35$  with  $T_{1N} \approx 1$  day as presented in Fig. 2A. Further SRSs did not result in any additional polarization build-up making us unable to obtain the HNPP in these samples.

In our experiments at Texas A&M University, we studied five TXS  $\text{H}_2$  samples with a thickness of  $10\text{--}100\mu\text{m}$ , four of them prepared from normal (75% ortho  $\text{H}_2$ , 25% para) and one from  $\approx 100\%$ -para hydrogen. The rf discharge had been run for a time period of 5–7 days and was stopped when the local H atom concentrations leveled off at  $\approx 10^{19}\text{cm}^{-3}$  (Fig. 3A and B), corresponding to those obtained for the TUS H- $\text{H}_2$  samples. The ESR spectra of H atoms obtained were non-symmetric and each line could be deconvoluted as a sum of two Lorentzian lines: a narrow component C1 and a broad component C2 (see Fig. 4A–C).

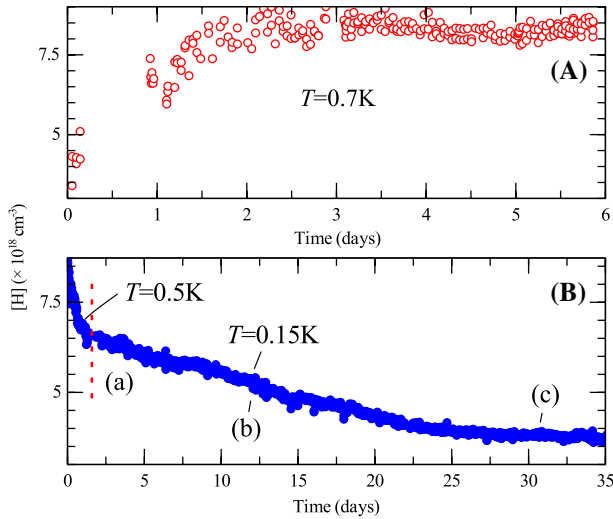


**Fig. 3** **A** Evolution of averaged local concentration of H atoms after starting the rf discharge for a H-H<sub>2</sub> TX sample. **B** Evolution of averaged local concentration of H atoms after stopping the rf discharge for H-H<sub>2</sub> in the same sample. The corresponding ESR spectra measured at different storage times are presented in Fig. 4 (Color figure online)

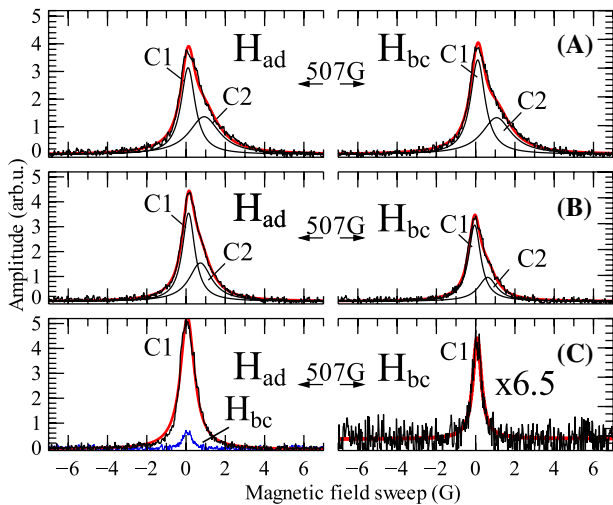


**Fig. 4** ESR spectra obtained at different storage times of the measurement presented in Fig. 3B. **A** ESR spectra of H in H<sub>2</sub> after stopping the discharge ( $T \approx 0.7$  K), **B** After cooling to 0.15 K but before sample became highly polarized, **C** At 0.1 K after establishing the HNPP. In Fig. 4C, the  $H_{bc}$  line is shown by a blue trace together with the  $H_{ad}$  line for comparison. Note that Component 2 disappeared when the highly polarized phase was attained. The fitting lines are shown as red lines in (C). The sums of the fitting lines are shown as red lines in (A) and (B) (Color figure online)

In contrast to the TUS, where we did not condense helium into the sample cell, reaching temperatures below  $\approx 0.5$  K after stopping the discharge in Texas required careful evacuation of the He gas from the sample cell which took more than  $\approx 20$  hours (Fig. 3B). Storing  $H_2$  films at this elevated temperature resulted in recombination of 20–25% of the initially accumulated H atoms and also led to conspicuous ESR line narrowing. While the width of the narrow Component 1 changed insignificantly from 0.85 G to  $\approx 0.75$  G, the width of the broader Component 2 decreased by 30% and amounted to 1.3 G (Fig. 4B). The ESR lines after cooling down to  $T \sim 0.15$  K were homogeneously broadened and the initial local H atom densities corresponding to both components presented in Fig. 4A were equal to  $4 \times 10^{18} \text{ cm}^{-3}$  (Component 1) and  $7 \times 10^{18} \text{ cm}^{-3}$  (Component 2), respectively. The concentrations of atoms corresponding to Components 1 and 2 at  $T=0.15$  K shown in Fig. 4B were  $\approx 3 \times 10^{18} \text{ cm}^{-3}$  and  $6 \times 10^{18} \text{ cm}^{-3}$ , respectively.

After evacuation of He gas from the SC had been completed, we proceeded to study the spontaneous polarization build-up of H atoms which took 5–7 days. The spontaneous nuclear polarization (SNPP) build-up was measured in four different samples stored at  $T=0.15$ , 0.3, 0.47 and 0.62 K, respectively (Fig. 5A). After storing the sample for one week, we equalized the populations of the  $|a\rangle$  and  $|b\rangle$  levels by saturating the  $H_{ab}$  NMR transition and then monitored the polarization recovery. Finally, we used the Overhauser effect DNP to ascertain that the HNPP could be created in this sample. We used a single SRS which increased the asymptotic polarization to  $p=0.46$  with a characteristic time  $T_{1N} \approx 2$  days. We found that the HNPP could be obtained by further application of SRSs. The results of those measurements are presented in Fig. 6A.

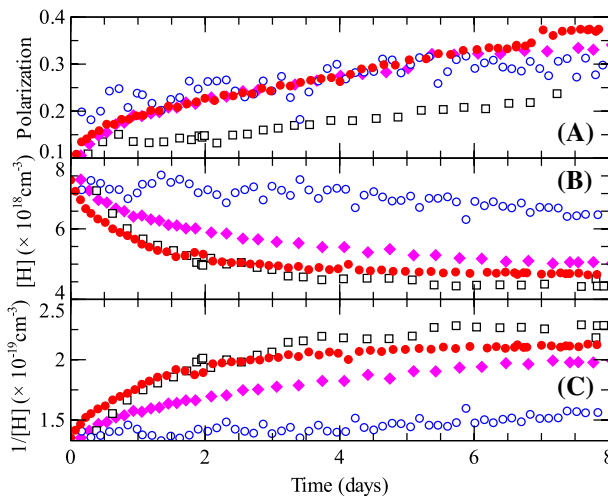


**Fig. 5** **A** Spontaneous evolution of nuclear polarization of H atoms in TXS and measured at  $T=0.15$  (open blue circles),  $T=0.3$  K (open black squares),  $T=0.47$  K (filled red circles) and  $T=0.62$  K (filled magenta diamonds). **B** Time evolution of average local concentrations for the same samples. **C** The inverse concentrations of H atoms as a function of time for the same measurements (Color figure online)

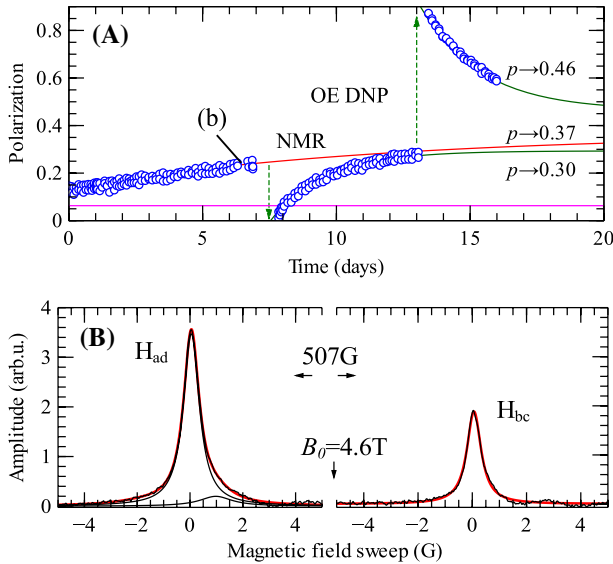


**Fig. 6** Spontaneous evolution of H atom nuclear polarization for the Texas data at  $T=0.3$  K followed by nuclear relaxation after saturating  $H_{ab}$  NMR transition and applying Overhauser effect DNP. Note that the  $T_{1N}$  time is much shorter than the characteristic time for the spontaneous nuclear polarization build-up. The time for measuring the ESR spectra shown in B is marked as (B) in (A). **B** The ESR lines of H atoms after establishing the SNPP for a TXS. The fitting lines are shown by red lines in (B) (Color figure online)

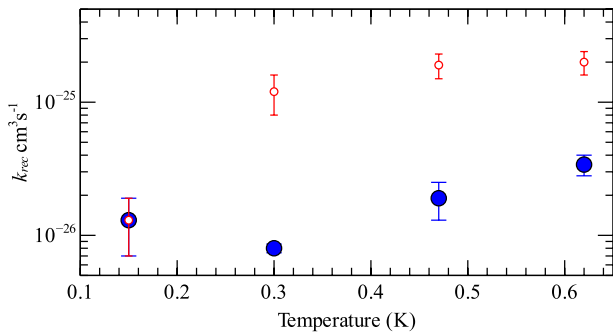


**Fig. 7** Recombination rates,  $k_{rec}$ , of H in  $H_2$  films studied in Texas for different temperatures estimated for the beginning ( $t < 2$  days) of storage (small red open circles) and for  $t > 2$  days (large blue-filled circles) for the measurements presented in Fig. 5 (Color figure online)

Storing the samples at  $T < 0.6$  K after stopping the rf discharge always resulted in the disappearance of the broad ESR line component which made the line shape nearly Lorentzian (Fig. 4C). In contrast to previous studies [8, 9], where atomic recombination was substantially suppressed at  $T=0.15$  K, in these studies the total number of atoms decreased by 10–15% during sample storage at this temperature for a time period of one week. The spontaneous build-up of H atom nuclear polarization and evolution of the averaged local concentrations of H atoms in solid  $H_2$

samples stored at  $T=0.15, 0.3, 0.47$  and  $0.62$  K are presented in Fig. 5A and B. The H atom recombination in solid  $H_2$  is a second-order process and the plots of inverse concentration as a function of time should be a linear function with the slopes of  $2k_r$ , where  $k_r$  is the H atom recombination rate. However, the time dependence of inverse H atom concentration for the TXS (Fig. 5C) had two regions of fast and slow recombination, respectively. The fast recombination at the beginning of sample storage,  $t < 2$  days, corresponds to mostly recombination of H atoms forming the broad C2 component, while the slow process takes over later when the H atom ESR lines contained only the C1 component. Dependencies of recombination rates of H atoms on temperature are shown in Fig. 7.

The H atom nuclear polarization after saturating the  $H_{ab}$  NMR transition recovered with a characteristic time of about 2 days as shown in Fig. 6A which is much faster than that for the initial SNPP build-up, about 10 days. This implies a possible memory effect similar to that observed for the HNPP in our previous work [19]. On the contrary, we did not observe a clear memory effect for the SNPP in TUS where the polarization recovery after saturating the  $H_{ab}$  transition took place with  $T_{1N}=1$  day in a fashion similar to that of the initial SNPP build-up (see Fig. 2A).

The spontaneous nuclear polarization for all four TXS measured at different temperatures approached  $p \simeq 0.35$  (see Fig. 5A) in accordance with that described in our previous work [19]. We did not observe any decay of the H atom nuclear polarization similar to that in the TUS. The H atom ESR spectra corresponding to the SNPP taken at  $T=0.15$  K are presented in Fig. 6B. The ESR lines had a Lorentzian shape and contained only one component except for a small broad component on the  $H_{ad}$  line corresponding to C2, visible during H atom accumulation and in the beginning of sample storage as presented in Fig. 4A and B. The SNPP build-up at  $T=0.47$  and  $0.62$  K took place faster as compared with that at  $T=0.3$  and  $0.15$  K. The H atom recombination at  $T=0.15$  K was also significantly slower than that at higher temperatures (Figs. 5B and 7). The asymptotic H atom nuclear polarization,  $p \simeq 0.35$ , was the same for the samples stored at different temperatures where the fraction of recombined H atoms was also different (Fig. 5B). Therefore, we may conclude that the spontaneous polarization build-up does not result from the preferential recombination of H atoms in the  $|b\rangle$ -state.

After the SNPP build-up had been measured, we applied 5–7 SRSs in order to reach the HNPP. This allowed achievement of the HNPP after about 2–3 weeks. The H atom ESR spectra corresponding to the HNPP were presented in Fig. 4C. Note the very high polarization achieved.

### 3.2 Effect of Magnetic Field

In our previous experiments carried out at Texas A&M University [19], we observed a drastic effect of magnetic field on the HNPP which was destroyed after completely discharging the magnet. In the present work, we studied the magnetic field effect on the HNPP and SNPP for the Texas samples and on the SNPP for the Turku samples where we were unable to obtain the HNPP. We investigated the effect of magnetic field on the nuclear polarization in two TUS, where  $H_2$  films were deposited directly

on the top Pd electrode of the quartz microbalance on the lower mirror without pre-plateing it with neon.

The first sample was stored at  $T=0.15$  K in a magnetic field of  $B=4.6$  T with an occasional application of DNP and short-term measurements at temperatures 0.1–1.5 K. Once the SNPP in the sample had been established, we fully discharged the magnet and kept the magnetic field at zero for 24 hours. Then the magnet was charged back to 4.6 T and the nuclear polarization measurement was resumed. Reducing magnetic field to zero decreased the nuclear polarization from  $p=0.35$  to  $p \approx 0.12$  which we measured after charging the magnet back to 4.6 T. The latter value is reasonably close to that for the Boltzmann occupation of the  $|a\rangle$  and  $|b\rangle$  states in a zero magnetic field,  $p=0.07$ , at  $T=0.15$  K. The nuclear polarization eventually recovered back to  $p \approx 0.35$  with a characteristic time  $T_{1N}=1$  day. The nuclear polarization after storing the sample for three days at  $B=2.2$  T decreased from  $p=0.32$  to  $p \approx 0.2$  and then recovered back to  $p \approx 0.27$  with the same characteristic time  $T_{1N}$ . We present a long-term evolution of the H atom nuclear polarization, both

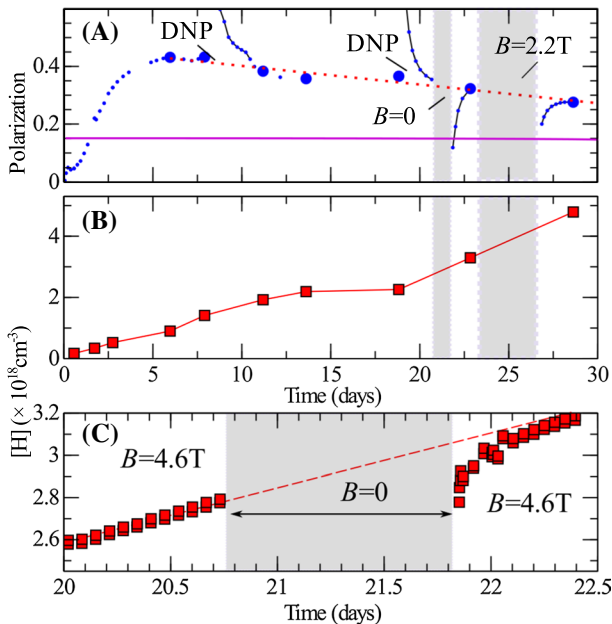


**Fig. 8** **A** Time evolution of the nuclear polarization of H atoms in a  $2.5 \mu\text{m}$  Turku sample at  $T=0.15$  K (blue dots). The asymptotic nuclear polarization is shown as blue-filled circles. The operations made with the samples are described by the labels. The experimental magnetic field if not specified separately is  $B=4.6$  T at which field the ESR data can be obtained. The H nuclear polarization corresponding to Boltzmann statistics at  $T=0.15$  K is shown by a solid magenta line. **B** Time evolution of the H atom concentrations for the same sample. The plateau in sample concentrations at  $t=15$ – $20$  days corresponds to measuring polarization at temperatures 0.1–1.5 K temperatures described in Section C (Effect of temperature). The time periods where magnetic field was reduced from 4.6 to 0 and 2.2 T are highlighted by gray rectangular shading. **C** Time dependence of H atom concentration which includes a period when magnetic was set to zero. The dashed red line shows the H atom growth rate expected at  $B=4.6$  T. The dotted and solid red lines in (A) are guides for the eye (Color figure online)

instantaneous (small blue dots in Fig. 8A) and asymptotic (blue-filled circles in the same figure), and the H atom concentrations for this 2.5  $\mu\text{m}$  H-H<sub>2</sub> sample (Fig. 8B). The plateau in Fig. 8B at  $t=15\text{--}20$  days since the beginning of Sample 1 storage corresponds to measuring polarization at temperatures 0.1–1.5 K described in Section C (Effect of temperature) and Fig. 8 caption.

The asymptotic nuclear polarizations measured in this sample at  $T=0.15$  K first rose in the beginning of sample storage and then started decaying slowly as shown in Fig. 8A. The application of DNP and magnetic field change did not influence the slope of H atom nuclear polarization decline in Fig. 8A. Therefore, we concluded that although the magnetic field disruption breaks the SNPP, it can be restored with a characteristic time equal to  $T_{1N}=1$  day.

The reduction of magnetic field to zero and charging it back to 4.6 T influenced the ESR line widths and integrals, the values we use to calculate a number of H atoms and their local concentrations in the sample. The calculated H atom concentration after charging the magnet back to  $B=4.6$  T appeared to be smaller at  $t=21.85$  days than that expected if the sample was stored at  $B=4.6$  T. An estimated evolution of H atom concentration at  $B=4.6$  T is shown in Fig. 8C by the dotted red line. A future study may provide more evidence on whether this reduction and fast recovery of H atom concentration after charging the magnet back to 4.6 T is related to a change of H atom recombination rate or is a mere instrumental effect.

For the second TUS, we carried out a similar experimental procedure. After the SNPP was created, we reduced the magnetic to 1.5 T and stored the sample for one day at this condition. After that, we charged the magnet back to 4.6 T and measured the polarization behavior. Following that we repeated this measurement sequence for  $B=3$  T. Similar to the first sample, nuclear polarization right after charging the magnet back to 4.6 T was close to that dictated by the Boltzmann statistics at the fields of 1.5 and 3 T, respectively. The nuclear polarization after charging the magnet recovered to the values  $p \approx 0.35$  with a characteristic time  $T_{1N}=1$  day, while slowly declining with the same slope as for the first sample.

In the Texas experiments we also studied the effect of magnetic field on the SNPP and HNPP established in the samples. When only the SNPP was formed prior to reducing the magnetic field to zero, the nuclear polarization recovered to  $p=0.37$  with a characteristic time of 2.5 days, equal to  $T_{1N}$ , which is shorter than the characteristic time of the SNPP build-up for the beginning of sample storage,  $\approx 7$  days.

The influence of magnetic field on the HNPP was further studied by carrying out two consecutive measurements at  $T=0.15$  K. In the first measurement, the sample was stored at  $B=4.6$  T. At the second set of measurements after the measurement at  $B=4.6$  T, we reduced the magnetic field to zero for 24 hours and the polarization recovery was measured after charging the magnet back to  $B=4.6$  T. The nuclear polarization right after recovering the field to  $B=4.6$  T was at the level of  $p=0.07$  (Fig. 9A) and then gradually increased during the course of sample storage in a magnetic field to an asymptotic value of  $p=0.49$  with the characteristic time of 7 days. In a second sequence we could achieve the HNPP again in this sample with *only one* SRS [19]. We did not observe any atomic recombination after discharging the magnet in either measurement for the TXS. The time evolution of local H atom

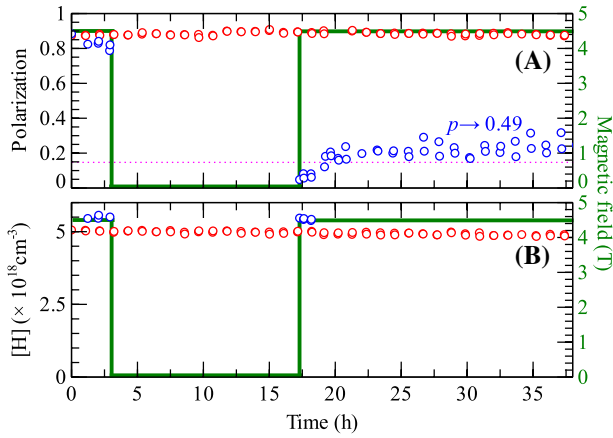


**Fig. 9** **A** Time evolution of the nuclear polarization and **B** the H atom concentration after reaching the HNPP and storing the sample at  $T=0.15$  K and  $B=4.6$  T (open red circles) and for the case of temporarily discharging the magnet to  $B=0$  (open blue circles). Note that in contrast to the nuclear polarization, the H atom concentration does not change in both measurements. The nuclear polarization expected on the basis of Boltzmann statistics is illustrated by the horizontal dotted magenta line in **A**. Magnetic field as a function of time for the case of temporarily discharging the magnet is shown by solid green lines (Color figure online)

concentration in the sample during storage at  $T=0.15$  K in magnetic field  $B=4.6$  T and after reducing magnetic field to zero are presented in Fig. 9B.

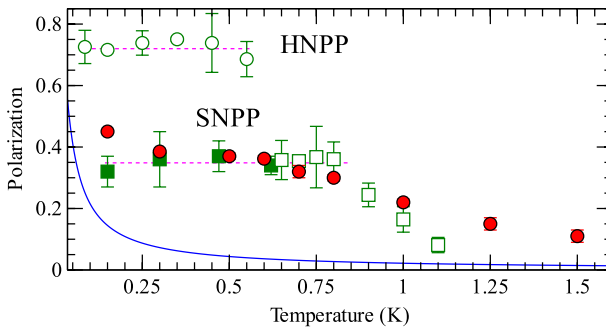


**Fig. 10** Temperature dependence of the nuclear polarization of H atoms in a  $2.5 \mu\text{m}$   $\text{H}_2$  TUS after establishing the SNPP (red circles). The asymptotic polarization corresponding to the SNPP and measured in a previous work done in Texas [19] by applying saturation-relaxation sequences (open green squares) and during spontaneous build-up in both this work and previous work [19] in Texas (filled green squares). The asymptotic polarization HNPP obtained by applying saturation-relaxation sequences in previous work done in Texas [19] are shown by open green circles. The H atom nuclear polarization as a function of temperature for Boltzmann statistics is shown by a solid blue line (Color figure online)

### 3.3 Effect of Temperature

In our previous work, we observed that the SNPP in fact remains stable in the temperature range 0.1–0.8 K for the TXS. In the present work, we studied the asymptotic nuclear polarization as a function of temperature after the SNPP had been formed in the Turku samples. The asymptotic polarization was measured by increasing the sample cell temperature in steps without applying DNP (Fig. 10). The lowest two temperature points (0.15 and 0.3 K), where the  $T_{1N}$  time was  $\approx 1$  day, were measured within about two days. The measurement times for the higher temperatures, where  $T_{1N}$  became shorter, were decreased to one day. The results of this measurement are shown by red circles in Fig. 10. We observed that the nuclear polarization corresponding to the SNPP is independent of temperature in the region of 0.15–0.6 K and remains at the level of  $p \approx 0.35$ . Raising temperature further resulted in a gradual decrease of the asymptotic polarization which approached the values corresponding to the Boltzmann statistics.

The asymptotic nuclear polarization as a function of temperature measured previously [19] for a TXS by applying SRSs after creating the HNPP is shown for comparison by open green squares in the temperature range 0.6–1.1 K. The nuclear polarizations built up spontaneously in the TXS studied in this and previous work [19], both corresponding to the SNPP are shown by filled green squares. The two sets of data corresponding to the SNPP measured in Turku and Texas show a quite similar dependence of the asymptotic polarization on temperature.

### 3.4 Substrate Effect

In our previous work [9], we did not observe any deviation from the Boltzmann statistics for the H atom nuclear polarization in 30 nm thick  $H_2$  films prepared on the upper copper mirror of the Fabry–Perot resonator (Fig. 1B and C). In this work, we made a special effort to study the effect of substrate on polarization by measuring the H atom nuclear polarization in TUS grown on the Pd bottom flat mirror as a function of the  $H_2$  film thickness. In addition to the 2.5  $\mu m$   $H_2$  film grown on top of

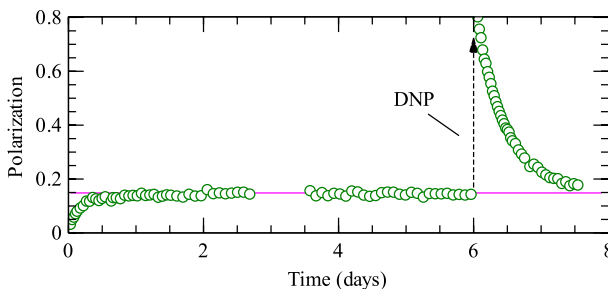


**Fig. 11** Evolution of H atom nuclear polarization in a 200 nm  $H_2$  film deposited on the Pd QM electrode studied in Turku and stored at  $T=0.15$  K when both methods, the rf discharge and bombardment by electrons released during tritium decay, were used for H atom production. The value of the nuclear polarization,  $p=0.15$ , for the Boltzmann occupation of the  $|a\rangle$  and  $|b\rangle$  states is shown by a solid magenta line (Color figure online)

the 2.5  $\mu\text{m}$  Ne film discussed above where the formation of the SNPP was observed, we studied a thinner, 200 nm thick  $\text{H}_2$  film deposited directly onto the Pd QM electrode. In order to accelerate the H atom accumulation, we also ran the rf discharge in the sample cell which was turned off when the H atom concentration approached  $2 \times 10^{19} \text{cm}^{-3}$ . The  $\text{H}_2$  film was also continuously bombarded by electrons released during decay of tritium from the sample cell walls.

Time evolution of H atom nuclear polarization in this latter thin sample is presented in Fig. 11. Similar to the results reported in our previous work [9] for H atoms in a 30 nm  $\text{H}_2$  film deposited on the copper spherical mirror, the H atom nuclear polarization in this sample did not deviate from the Boltzmann statistics as shown in Fig. 11. Applying the Overhauser effect DNP did not increase the nuclear polarization which returned to the level of  $p \approx 0.15$  after relaxation. In addition, we also studied the H atom nuclear polarization build-up in a 160 nm Turku  $\text{H}_2$  film deposited on the Pd mirror preplated with a 1  $\mu\text{m}$  solid Ne film. In this case, the SNPP with  $p=0.30$  was achieved in the course of sample storage for four days.

In contrast to the samples created on the Mylar coated mirror studied in Texas, where we were able to create both nuclear-polarized phases, we failed to observe any  $|a\rangle$ -state overpopulation for the H atoms in the  $\text{H}_2$  films deposited on the metallic spherical ESR mirror in Texas. It might be expected that the  $\text{H}_2$  film formed on the spherical mirror has a thickness of  $\approx 100$  nm where the H atoms are produced during the rf discharge. The substrate effects for such thin films may lead to fast relaxation and prevent the nuclear polarization build-up.

## 4 Discussion

In this work, we have presented an experimental study of the nuclear polarization of H atoms stabilized in solid  $\text{H}_2$  matrices. The two types of H- $\text{H}_2$  samples were created using different deposition and dissociation techniques. The TUS  $\text{H}_2$  films were quench-condensed onto a cold metallic QM surface and had a thickness of 0.2–2.5  $\mu\text{m}$ . The  $\text{H}_2$  films created on the Mylar surface at Texas A&M were 10–100  $\mu\text{m}$  thick. The dissociation techniques were also markedly different. The former films were exposed to a continuous bombardment by 5.7 keV electrons released during  $\beta$ -decay of tritium trapped in the sample cell walls, while the H atoms in the latter samples were generated by low-energy electrons from running the rf discharge in He vapor above the solid  $\text{H}_2$  film.

First, we summarize the main results and the differences in the build-up of H atom nuclear polarization for the two types of samples. The TUS, where observations were made under conditions such that the H atom generation could not be stopped, behaved differently from the TXS where the H atom observations were made after the H atom accumulation was stopped by turning off the discharge. The nuclear polarization in the TUS increased during the first few days of storage and after achieving the maximum H atom nuclear polarization at  $p \approx 0.42$  then experienced a steady decline which was not influenced by disrupting the magnetic field. The steady state polarization then approached  $p \approx 0.35$ , similar to that observed for the SNPP in the TXS of the present work and the samples studied earlier [19].

However, we were not able to create the HNPP of H atoms in the TUS. The characteristic times for achieving the SNPP in Turku and Texas samples were also markedly different, about 2 and 5–10 days, respectively. The polarization recovery after saturation of the  $H_{ab}$  NMR transition in the Texas experiment took place with a clearly shorter characteristic time compared to that of the spontaneous polarization build-up. This provides evidence for a memory effect and implies preservation of a specific spatial arrangement of H atoms in the  $H_2$  matrix associated with the SNPP. A similar memory effect was observed for the HNPP in our previous work [19]. However, we did not observe a clear memory effect in the TUS. The absence of the HNPP in the TUS might also be related to the absence of such an arrangement of H atoms. One of the possibilities for a spatial arrangement might be related to the aggregation of H atoms near the lattice defects or near the surface. A higher mobility of H atoms in the TUS may suppress the formation of such a spatial arrangement of H atoms which may also prevent the formation of HNPP in these samples. Further studies are required to probe for the possibility of spatial aggregation of H atoms in solid  $H_2$ .

In contrast to the Turku samples where the H atom ESR lines were Lorentzian and contained only one component, the ESR lines of H atoms in the TXS right after stopping the H atom accumulation, contained two components, C1 and C2 (see Fig. 4A). The HNPP in the TXS was established only after the broader C2 component disappeared.

Previously, we attributed the composite H atom ESR line shape for atoms created by running the rf discharge in the sample cell to the regions with different local H atom concentrations [10]. The low-energy electrons in these studies dissociated  $H_2$  molecules only in a rather shallow surface layer (about 100 nm) of the 10–100  $\mu\text{m}$  thick  $H_2$  films. We suggested that the broader component corresponded to H atoms at higher concentration closer to the film surface and the narrow one was related to the H atoms residing in more dilute regions deeper in the  $H_2$  film bulk. In Turku samples, high-energy electrons produced during tritium decay uniformly dissociate  $H_2$  molecules in the 2.5  $\mu\text{m}$  solid hydrogen films, without creating concentration gradient in the film. A regular Lorentzian shape of the H atom ESR lines in Turku samples supports our earlier conclusions on the component assignment.

Now we proceed to the discussion of the most peculiar characteristics of the Turku H- $H_2$  samples: the absence of the HNPP phase and the gradual decrease of the sample polarization for the 2.5  $\mu\text{m}$  thick  $H_2$  samples deposited directly on the bare mirror and after preplating it with a 2.5  $\mu\text{m}$  Ne film as well as the Boltzmann behavior of H atom nuclear polarization in 160 nm thick  $H_2$  films deposited directly onto the bare Pd ESR mirror. The possible reasons for a different behavior of the H atom nuclear polarization in the TXS and TUS could be the difference in the dissociation techniques we utilized, substrate materials and sample thicknesses.

The electrons which continuously bombard the  $H_2$  films in TUS created a large number of phonons which stimulate the H atom nuclear spin relaxation. Faster relaxation may prevail over the polarization build-up mechanism, tending to restore the Boltzmann occupation for energy levels of H atoms. We were also unable to observe any overpopulation of the  $|a\rangle$ -state while running the discharge in the sample cell

at temperatures of 0.6–0.8 K in our experiments in Texas as well as in the previous studies.

Moreover, the TUS were created on a metal substrate and the H atoms were generated uniformly in the whole film volume. In contrast to that, the TXS were much thicker and the H atoms were generated only in a very thin ( $\approx 100$  nm) surface layer. Therefore, it might be suggested, that the substrate effects may still play a role for the TUS. The metal substrate may facilitate nuclear spin relaxation which can efficiently reduce the observed values of nuclear polarization. The  $T_{1N}$  times measured in the TUS are nearly an order of magnitude shorter than those in TXS. The nuclear relaxation of H atoms near the substrate can be enhanced due to conduction electrons in the metal substrate. These quickly relaxing H atoms at the Pd/H<sub>2</sub> interface may first trigger nuclear relaxation of the H atoms residing nearby and then reduce the nuclear polarization of more remote H atoms in the sample by means of spin diffusion. This may also explain the absence of high nuclear polarization in earlier experiments [9] with H atoms in thin H<sub>2</sub> films (30 nm) grown on the Mylar substrate for samples where the discharge was run using the rf-resonator arranged in a close vicinity to the substrate. On the contrary, high nuclear polarizations were observed for the H atoms created using the rf coil located further away from the H<sub>2</sub> film. It might be suggested, that in the former case a large number of free radicals or other quickly relaxing centers which might stimulate the H atom nuclear relaxation were created in the substrate due to the discharge. The formation of high nuclear polarization in the latter case might be due to the absence of such quickly relaxing centers created in the Mylar substrate. The H atom concentrations in these two samples were also different,  $2 \times 10^{19}$  and  $2 \times 10^{18} \text{cm}^{-3}$ , respectively. However, we did not observe a clear influence of the sample concentration on the possibility of building up high nuclear polarization of H atoms. The high nuclear polarization was also observed for thin H<sub>2</sub> films grown on the Mylar substrate during the three-body recombination of H atoms in the gas phase [8]. In this case, no rapidly relaxing centers in the Mylar film were created which might have stimulated the relaxation of H atoms in the H<sub>2</sub> film. This conclusion is also supported by SNPP build-up in thin H<sub>2</sub> films grown on the Pd mirror preplated with a 1  $\mu\text{m}$  Ne film.

The H atoms in the TXS initially reside in a  $\approx 100$  nm surface layer and remain spatially isolated from the substrate which cannot influence relaxation of the H atom nuclear spins. The nuclear relaxation in 160 nm Turku samples is a factor of 2–3 faster than that in the 2.5  $\mu\text{m}$  films. It might be suggested that the asymptotic nuclear polarization observed experimentally is a result of the competition between the polarizing mechanism and nuclear relaxation. Therefore, a smaller asymptotic polarization might be expected for a shorter  $T_{1N}$  time. Thus, one might conclude that the faster nuclear relaxation may suppress the SNPP formation in thin H<sub>2</sub> films. It is also important to emphasize that the nuclear-polarized phases were observed in samples studied in Texas made of both normal and para-H<sub>2</sub> gases.

In our previous work [19], we suggested that one of the possible mechanisms for a gradual nuclear polarization build-up may be alignment of H atom nuclear spins due to their interaction via the  ${}^3\Sigma_u^+$  potential with a possible formation of weakly bound triplet H<sub>2</sub> molecules. In this case, faster relaxation may compensate for the

H atom nuclear polarization build-up and reduce the values of the polarization observed experimentally.

## 5 Conclusions

To summarize, in this work we reported on the results of two joint experiments at the University of Turku and Texas A&M University on studying the nuclear-polarized phases of H atoms in solid H<sub>2</sub> matrices. The solid H<sub>2</sub> films in these experiments were formed using two different techniques: quench condensation of thin 0.2–2.5 μm thick H<sub>2</sub> films onto a cold substrate in the Turku experiments and solidification of thick (10–100 μm) H<sub>2</sub> films from the liquid phase in the Texas experiments. The H atoms in the Texas and Turku experiments were created by running an rf-discharge and bombarding the solid H<sub>2</sub> films by 5.7 keV electrons generated during decay of tritium trapped in the sample cell walls, respectively.

We observed a robust effect of the formation of a spontaneous nuclear polarized phase of hydrogen atoms,  $p=0.35$ , in numerous experiments where hydrogen atoms embedded in solid molecular hydrogen samples were well isolated from the influence of the substrate. This effect does not depend on the sample preparation techniques, which include different H<sub>2</sub> film depositions and the dissociation methods for converting molecules to atoms.

In thick molecular films grown via the solidification process, the nuclear polarization could be further increased by repeated action of Dynamic Nuclear Polarization followed by relaxation to a steady state with even a larger nuclear polarization, leading to formation of the highly nuclear-polarized phase,  $p=0.75$ . As a possible explanation for developing both types of hyperpolarization, we proposed the formation followed by dissociation of weakly bound triplet hydrogen molecules, leading to a production of an excessive population of hydrogen atoms in the lowest energy  $a$ -state [19, 21]. This process, competing with the nuclear relaxation, results in a steady state with a population of the hyperfine  $a$ -state substantially larger than that dictated by the Boltzmann statistics.

The highly nuclear-polarized phase was not observed in the Turku experiments with fairly thick H<sub>2</sub> films prepared by cold molecular epitaxy followed by dissociation with fast 5.7 keV electrons. This different behavior appears as a result of faster nuclear spin-lattice relaxation due to continuous exposure of H<sub>2</sub> films to electrons released in tritium decay in the cell walls. In the Turku experiments, nuclear relaxation might be further enhanced by the quickly relaxing centers created in the substrate during continuously accumulation of H atoms in the thin H<sub>2</sub> films.

Slow spontaneous growth of H atom nuclear polarization in high magnetic fields was observed for all thick samples and proceeded with the characteristic time an order of magnitude larger than the time of nuclear relaxation. This indicates slow structural changes of the H-H<sub>2</sub> films leading to formation of regions with spatial aggregations of H atoms or migration of atoms into the regions far from the lattice defects. Spatial aggregation of H atoms can also explain the observed effects of faster recovering of polarization after switching off and on the magnetic field. The

additional quantum overlap achieved when this spatial aggregation occurs can help to build the observed nuclear magnetic phases. This sensitivity to shorter nearest neighbor distances is a sign that at substantially higher concentrations, Bose-Einstein condensation of hydrogen atoms on a larger scale might occur. Further studies of this phenomenon may help to clarify the underlying physics.

This article is prepared for a Special Issue devoted to the 90th birthdays of great scientists and friends, David M. Lee and John D. Reppy. The authors of this article have had long-term collaborative work with David Lee. Working with David Lee has always been very interesting, enjoyable, and fun. He is still active in low-temperature physics, performing experiments using electron spin resonance and optical spectroscopy on atoms trapped in thin films and in porous media at low temperatures. This article is the result of a collaborative effort by the group at Texas A&M University, USA, led by David Lee and the group from the University of Turku, Finland, headed by Dr. Sergey Vasiliev for investigation of the properties of the recently discovered nuclear magnetic phases of hydrogen atoms embedded in solid molecular hydrogen.

**Acknowledgements** This work has been supported by National Science Foundation Grant No. DMR 2104756, Academy of Finland Grant No. 317141, and Office of the Naval Research Grant N00014-20-1-2184.

**Data Availability Statement** Data are available on reasonable request

## Declarations

**Conflict of interest** The authors declare that they have no conflict of interest.

## References

1. A.Y. Katunin, I.I. Lukashevich, S.T. Orozmatov, V.V. Sklyarevskii, V.V. Suraev, V.V. Filippov, N.I. Filippov, V.A. Shevtsov, Temperature dependence of the recombination rate constant of hydrogen atoms in solid H<sub>2</sub> at 1.5 K < T < 5.5 K. *JETP Lett.* **34**, 357 (1981)
2. A.V. Ivliev, A.Y. Katunin, I.I. Lukashevich, V.V. Sklyarevskii, V.V. Suraev, V.V. Filippov, N.I. Filippov, V.A. Shevtsov, Temperature dependence of quantum diffusion of H atoms in solid H<sub>2</sub> in the temperature range 1.35 K <= T <= 4.2 K. (1982)
3. E.B. Gordon, A.A. Pel menev, O.F. Pugachev, V.V. Khmelenko, Hydrogen and deuterium atoms, stabilized by condensation of an atomic beam in superfluid helium. *JETP Lett.* **37**(5), 282 (1983)
4. T. Miyazaki, K.P. Lee, K. Fueki, A. Takeuchi, Temperature effect on the decay of hydrogen (deuterium) atoms in the radiolysis of solid molecular hydrogen, molecular deuterium, and hydrogen-deuterium molecule (HD) at 4.2 and 1.9 K. Evidence for tunneling migration. *J. Phys. Chem.* **88**(21), 4959 (1984)
5. T. Miyazaki, N. Iwata, K.P. Lee, K. Fueki, Decay of hydrogen(deuterium) atoms in solid hydrogen at 4.2 K: rate constant for tunneling reaction hydrogen (deuterium, hydrogen deuteride) + hydrogen (deuterium) atom. *J. Phys. Chem.* **93**(8), 3352 (1989)
6. S.I. Kiselev, V.V. Khmelenko, D.M. Lee, Hydrogen atoms in impurity-helium solids. *Phys. Rev. Lett.* **89**, 175301 (2002)
7. T. Kumada, Experimental determination of the mechanism of the tunneling diffusion of H atoms in solid hydrogen: physical exchange versus chemical reaction. *Phys. Rev. B* **68**, 052301 (2003)

8. J. Ahokas, J. Järvinen, V.V. Khmelenko, D.M. Lee, S. Vasiliev, Exotic behavior of hydrogen atoms in solid H<sub>2</sub> at temperatures below 1 K. *Phys. Rev. Lett.* **97**(9), 095301 (2006)
9. J. Ahokas, O. Vainio, S. Novotny, J. Järvinen, V.V. Khmelenko, D.M. Lee, S. Vasiliev, Magnetic resonance study of H atoms in thin films of H<sub>2</sub> at temperatures below 1 K. *Phys. Rev. B* **81**, 104516 (2010)
10. J. Järvinen, V.V. Khmelenko, D.M. Lee, J. Ahokas, S. Vasiliev, Atomic Hydrogen in Thick H<sub>2</sub> Films at Temperatures 0.05–2 K. *J. Low Temp. Phys.* **162**(3), 96 (2011)
11. K.R.A. Hazzard, E.J. Mueller, Candidate theories to explain the anomalous spectroscopic signatures of atomic H in molecular H<sub>2</sub> crystals. *Phys. Rev. B* **82**, 014303 (2010)
12. E. Kim, M. Chan, Probable observation of a supersolid helium phase. *Nature* **427**, 225 (2004)
13. D.Y. Kim, M.H.W. Chan, Absence of supersolidity in solid helium in porous vycor glass. *Phys. Rev. Lett.* **109**, 155301 (2012)
14. A. Haziot, X. Rojas, A.D. Fefferman, J.R. Beamish, S. Balibar, Giant plasticity of a quantum crystal. *Phys. Rev. Lett.* **110**, 035301 (2013)
15. J.R. Li, J. Lee, W. Huang, S. Burchesky, B. Shteynas, F. Top, A.O. Jamison, W. Ketterle, Probable observation of a supersolid helium phase. *Nature* **543**, 91 (2017)
16. L. Tanzi, E. Lucioni, F. Famà, J. Catani, A. Fioretti, C. Gabbanini, R.N. Bisset, L. Santos, G. Modugno, Observation of a dipolar quantum gas with metastable supersolid properties. *Phys. Rev. Lett.* **122**, 130405 (2019)
17. F. Böttcher, J.N. Schmidt, M. Wenzel, J. Hertkorn, M. Guo, T. Langen, T. Pfau, Transient supersolid properties in an array of dipolar quantum droplets. *Phys. Rev. X* **9**, 011051 (2019)
18. L. Chomaz, D. Petter, P. Ilzhöfer, G. Natale, A. Trautmann, C. Politi, G. Durastante, R.M.W. van Bijnen, A. Patscheider, M. Sohmen, M.J. Mark, F. Ferlaino, Long-lived and transient supersolid behaviors in dipolar quantum gases. *Phys. Rev. X* **9**, 021012 (2019)
19. S. Sheludiakov, P.T. McColgan, D.M. Lee, V.V. Khmelenko, J. Järvinen, J. Ahokas, S. Vasiliev, Formation of nuclear-polarized phases of H atoms embedded in solid H<sub>2</sub> films. *Phys. Rev. Lett.* **122**, 225301 (2019)
20. S. Sheludiakov, J. Ahokas, J. Järvinen, D. Zvezdov, O. Vainio, L. Lehtonen, S. Vasiliev, S. Mao, V.V. Khmelenko, D.M. Lee, Dynamic nuclear polarization of high-density atomic hydrogen in solid mixtures of molecular hydrogen isotopes. *Phys. Rev. Lett.* **113**, 265303 (2014)
21. S. Sheludiakov, D.M. Lee, V.V. Khmelenko, J. Ahokas, J. Järvinen, S. Vasiliev, Studies of nuclear polarization of hydrogen atoms embedded in solid molecular hydrogen and hydrogen deuteride films. *Low Temp. Phys.* **46**(2), 139 (2020)
22. S. Vasilyev, J. Järvinen, E. Tjukanoff, A. Kharitonov, S. Jaakkola, Cryogenic 2 mm wave electron spin resonance spectrometer with application to atomic hydrogen gas below 100 mK. *Rev. Sci. Instrum.* **75**(1), 94 (2004)
23. S. Sheludiakov, J. Ahokas, O. Vainio, J. Järvinen, D. Zvezdov, S. Vasiliev, V.V. Khmelenko, S. Mao, D.M. Lee, Experimental cell for molecular beam deposition and magnetic resonance studies of matrix isolated radicals at temperatures below 1 K. *Rev. Sci. Instrum.* **85**(5), 053902 (2014)
24. S. Sheludiakov, J. Ahokas, J. Järvinen, L. Lehtonen, O. Vainio, S. Vasiliev, D.M. Lee, V.V. Khmelenko, ESR study of atomic hydrogen and tritium in solid T<sub>2</sub> and T<sub>2</sub>:H<sub>2</sub> matrices below 1 K. *Phys. Chem. Chem. Phys.* **19**, 2834 (2017)
25. S. Sheludiakov, J. Ahokas, J. Järvinen, L. Lehtonen, S. Vasiliev, Y.A. Dmitriev, D.M. Lee, V.V. Khmelenko, Electron spin resonance study of atomic hydrogen stabilized in solid neon below 1 K. *Phys. Rev. B* **97**, 104108 (2018)
26. A. Abragam, *The Principles of Nuclear Magnetism* (Clarendon Press, Oxford, 1961)